Ⓔ

# SPITZER IDENTIFICATIONS AND CLASSIFICATIONS OF SUBMILLIMETER GALAXIES IN GIANT, HIGH-REDSHIFT, Lyα-EMISSION-LINE NEBULAE

J. E. GEACH,[1] IAN SMAIL,[1] S. C. CHAPMAN,[2,3,4] D. M. ALEXANDER,[1] A. W. BLAIN,[4] J. P. STOTT,[1] AND R. J. IVISON[5]

## ABSTRACT

Using *Spitzer Space Telescope* IRAC (3.6–8 $\mu$m) and MIPS (24 $\mu$m) imaging, as well as *Hubble Space Telescope* optical observations, we identify the IRAC counterparts of the luminous power sources residing within the two largest and brightest Lyα-emitting nebulae (LABs) in the SA 22 protocluster at $z = 3.09$ (LAB 1 and LAB 2). These sources are also both submillimeter galaxies (SMGs). From their rest-frame optical/near-infrared colors, we conclude that the SMG in LAB 1 is likely starburst dominated and heavily obscured ($A_V \sim 3$). In contrast, LAB 2 has excess rest-frame $\sim 2$ $\mu$m emission (over that expected from starlight) and hosts a hard-X-ray-emitting active galactic nucleus (AGN) at the proposed location of the SMG, consistent with the presence of an AGN. We conclude that LAB 1 and LAB 2 appear to have very different energy sources despite having similar Lyα spatial extents and luminosities, although it remains unclear whether ongoing star formation or periodic AGN heating is responsible for the extended Lyα emission. We find that the mid-infrared properties of the SMGs lying in LAB 1 and LAB 2 are similar to those of the wider SMG population, and so it is possible that extended Lyα halos are a common feature of SMGs in general.

*Subject headings:* galaxies: active — galaxies: high-redshift — infrared: galaxies

*Online material:* color figures

## 1. INTRODUCTION

Narrowband surveys have revealed an intriguing new population: giant, radio-quiet, Lyα-emission-line nebulae (Steidel et al. 2000), which have been termed "Lyα blobs" (LABs). These objects typically have linear extents of 10–100 kpc and Lyα luminosities of $10^{43}$–$10^{44}$ ergs s$^{-1}$, with the highest concentration currently known in the SA 22 protocluster at $z = 3.09$, with 35 confirmed objects (Matsuda et al. 2004). Similar objects have been discovered in other regions associated with rich but primitive environments (Keel et al. 1999; Francis et al. 2001; Palunas et al. 2004), and extended Lyα emission has been detected around certain high-redshift radio galaxies (e.g., Reuland et al. 2003); however, the narrowband-selected LABs are typically not associated with such radio-loud systems.

Cooling flows or shock heating by outflows originating from starburst winds or AGN jets have been proposed as the most plausible mechanisms for producing these extended Lyα halos (Taniguchi & Shioya 2000; Ohyama et al. 2003), although other processes such as subsonic $p\,dV$ heating and inverse Compton scattering of Sunyaev-Zel'dovich photons could also play a role (Scharf et al. 2003). The two largest known LABs (LAB 1 and LAB 2, with spatial extents of $1.1 \times 10^4$ and $0.8 \times 10^4$ kpc$^2$, respectively, both at $z = 3.09$ in SA 22; Matsuda et al. 2004) are both associated with submillimeter galaxies (SMGs; Chapman et al. 2001). Several other LABs in the SA 22 structure at $z = 3.09$ contain SMGs (Geach et al. 2005); the apparent association of these bolometrically luminous galaxies with LABs provides support for the scenario in which feedback mechanisms are powering the Lyα emission, since the bolometric luminosities of the SMGs are several orders of magnitude larger than the Lyα luminosities of the halos. The

action of superwind feedback has recently been given credence by integral field data that reveal outflows and complex velocity structures in both LAB 1 and LAB 2 (Bower et al. 2004; Wilman et al. 2005). However, the precise location and identification of the SMG counterparts, and hence accurate constraints on the dominant power sources, are unclear due to the poor spatial resolution of the submillimeter data (Chapman et al. 2004).

In this Letter, we present *Spitzer Space Telescope* mid-infrared and *Hubble Space Telescope* (*HST*) optical imaging of the galaxies embedded within LAB 1 and LAB 2 to locate the bolometrically luminous sources within them: the SMGs. To identify these galaxies, we exploit the fact that mid-infrared observations have been shown to be effective at identifying SMGs, particularly at 8 $\mu$m since these galaxies have red infrared colors (Ashby et al. 2006). The mid-infrared photometry also constrains their rest-frame optical–radio spectral energy distributions (SEDs) and hence can shed light on what is powering these sources. Throughout we adopt $\Omega_m = 0.3$, $\Omega_\Lambda = 0.7$, and $H_0 = 75$ km s$^{-1}$ Mpc$^{-1}$. In this geometry, $1''$ corresponds to 7.1 kpc at $z = 3.09$.

## 2. OBSERVATIONS AND REDUCTION

The *Spitzer* observations used here are part of GTO project 64, which we retrieved from the *Spitzer* Science Center (SSC) archive. LAB 1 and LAB 2 are covered by all four IRAC channels (3.6–8 $\mu$m), and we use the Post Basic Calibrated IRAC frames generated by the pipelines at the SSC. Both LABs were also observed by MIPS at 24 $\mu$m as part of the same project, and for these data we perform postprocessing on Basic Calibrated Data frames to remove common MIPS artifacts and flatten small- and large-scale gradients using "master flats" generated from the data. For mosaicking we use the SSC MOPEX package, which makes use of the supplementary calibration files that are supplied with the main science set. We use SExtractor (ver. 2.4.4; Bertin & Arnouts 1996) to detect and extract sources in the mid-infrared images. Fluxes are measured in apertures with diam-

[1] Institute for Computational Cosmology, Durham University, UK; j.e.geach@durham.ac.uk.
[2] Institute of Astronomy, University of Cambridge, UK.
[3] Canadian Space Agency Fellow, University of Victoria, BC, Canada.
[4] California Institute of Technology, Pasadena, CA.
[5] Astronomy Technology Centre, Royal Observatory, Edinburgh, UK.

eters chosen to be the same as in the SWIRE ELAIS-N1 catalog:[6] 3.8″ for IRAC and 12″ for MIPS.

In addition to the mid-infrared data, we analyze optical *HST* observations of the LABs, to reveal the rest-frame ultraviolet (UV) morphologies of the galaxies in the LAB halos. The STIS coverage of LAB 1 has been previously discussed by Chapman et al. (2004), while the Advanced Camera for Surveys (ACS) F814W (*I* band) imaging of LAB 2 is presented here for the first time. The ACS data were reduced using Multidrizzle and will be described in more detail in J. E. Geach et al. (2007, in preparation).

## 3. IDENTIFICATION OF THE SMGs

As the precise location of the SMGs within the LAB halos is uncertain, we begin our discussion by identifying the mid-infrared counterparts to the SMGs (which we assume to be the dominant power source of the LABs). Starting with a catalog of the IRAC detections within each Lyα halo[7] (Table 1), we aim to eliminate sources not at $z = 3.1$ and then identify the most likely mid-infrared counterpart (if any) to the SMG in each case. Note that no sources are detected at 24 μm within the extent of either LAB, and so we adopt 3 σ upper limits of $f_{24} < 330$ μJy.

Figure 1 shows *HST* and IRAC images of the LABs covering 3.6–8 μm, and we label each of our potential counterparts. Of the five IRAC components in LAB 1 (a–e), we can eliminate several of them as the SMG counterpart immediately: LAB 1c and 1d have mid-infrared colors $f_{3.6}/f_{4.5} > 1$, making them inconsistent with $z = 3.1$ galaxies (Ashby et al. 2006), while LAB 1e is at the position of the Lyman break galaxy (LBG) C11, and is only weakly detected at 3.6 μm and undetected at 4.5–8 μm. Although this LBG is close to LAB 1, it appears to be kinematically distinct from the bulk of the halo (Bower et al. 2004) and so we discount it, leaving LAB 1a and 1b as potential counterparts.

The positional uncertainty between LAB 1a and the 850 μm centroid ($\Delta\theta = 2.0″ \pm 1.9″$) is consistent with its being the source of the submillimeter emission. The remaining IRAC counterpart to the southeast of the SMG (LAB 1b) is just within the Lyα halo and has a bright counterpart in the STIS imaging. It is not clear from the mid-infrared colors whether this galaxy is at the halo redshift, but given its large separation from the nominal submillimeter position, it is unlikely that it is associated with the power source. However, if LAB 1b is at $z = 3.1$, it is possible that LAB 1a and 1b are interacting given their projected separation of just ∼4″ (∼30 kpc at $z = 3.1$).

Previous multiwavelength observations of LAB 1 (Chapman et al. 2004) associated the SMG with the brightest of a group of UV fragments near the geometrical center of the structure and close to the 21 cm source position (Fig. 1). Component LAB 1a is in the vicinity of this group of faint UV fragments, but the 3.6–8 μm emission is coincident with a $K_s = 21.5$ extremely red object (ERO) identified in Steidel et al. (2000), rather than the brightest UV component ("J1" in Chapman et al. 2004), which is closest to the radio peak [and a tentative CO(4–3) detection]. Both LAB 1a and the UV object J1 are plausible sources of the submillimeter emission. However, given that SMGs are expected to be massive, we view the 3.6–8 μm detection as a more reliable indicator of the SMG's

### TABLE 1
### Mid-IR Properties of Sources Lying within LABs

| COMPONENT | OFFSETS (arcsec) Δα | Δδ | FLUX (μJy) 3.6 μm | 4.5 μm | 5.8 μm | 8.0 μm |
|---|---|---|---|---|---|---|
| LAB 1a ...... | 0.0 | 0.0 | 4.3 | 5.8 | <6.6 | 7.6 |
| b ........... | 1.5 | −3.4 | 5.5 | 7.3 | 7.6 | 7.9 |
| c ........... | 1.5 | 10.7 | 4.8 | 3.8 | <6.6 | <6.6 |
| d ........... | −3.0 | 7.7 | 2.8 | 1.9 | <6.6 | <6.6 |
| e ........... | −4.5 | −1.4 | 1.5 | <0.9 | <6.6 | <6.6 |
| LAB 2a ...... | 3.0 | −7.7 | 3.4 | 4.1 | <6.6 | <6.6 |
| b ........... | 0.0 | 0.0 | 3.8 | 5.0 | <6.6 | 9.2 |
| c ........... | −3.0 | −5.5 | 16.3 | 12.0 | 8.1 | <6.6 |

NOTES.—The positional offsets are from the SMGs in LAB 1 and LAB 2 identified in § 3. The proposed mid-infrared counterparts, LAB 1a and LAB 2b, are at $22^h17^m26.0^s$, $+00°12′36.2″$ and $22^h17^m39.1^s$, $+00°13′30.4″$ (J2000.0), respectively. Positional uncertainties based on the 3.6 μm centroids are 0.8″. The flux uncertainties are 0.3 μJy in 3.6 and 4.5 μm and 2.2 μJy in 5.8 and 8.0 μm. Quoted limits are 3 σ.

counterpart than the weak UV source. We therefore propose that LAB 1a is the most likely IRAC counterpart to the SMG in LAB 1.

There are three mid-infrared counterparts within the extent of LAB 2 (Fig. 1, Table 1). We can eliminate LAB 2c immediately as a potential counterpart given its blue mid-infrared colors and large, bright optical counterpart in the *HST* image; it is a foreground object. The remaining two counterparts LAB 2a and LAB 2b have similar 3.6–5.8 μm characteristics and similar compact *HST* morphologies (Fig. 1). However, only LAB 2b is detected at 8 μm, which has been shown to be a useful identifier of the mid-infrared counterparts of SMGs (Ashby et al. 2006). Moreover, LAB 2 contains a hard X-ray source in the halo (Basu-Zych & Scharf 2004), with an estimated luminosity $L_X \sim 10^{44}$ ergs s$^{-1}$. The location of the X-ray source is consistent with LAB 2b ($\Delta\theta = 0.8″ \pm 1.4″$), whereas LAB 2a is in the extreme southeast of the LAB, ∼8.5″ away from the X-ray source. Given the association between SMGs and moderately bright X-ray sources (Alexander et al. 2005b), the SMG in LAB 2 is likely to lie close to the position of the X-ray source. We therefore propose that LAB 2b is the mid-infrared counterpart to the SMG in LAB 2.[8] The precise positions of the SMGs in LAB 1 and LAB 2 and the offsets to the other mid-infrared components are given in Table 1.

## 4. CLASSIFICATION OF THE SMGs

We can use the 3.6–8 μm photometry (along with multiwavelength data for these objects from the literature; Chapman et al. 2001, 2004; Steidel et al. 2000) to construct the optical–radio SEDs for the SMGs (Fig. 2). We present new *J*- and *K*-band photometry from the UKIDSS Deep Extragalactic Survey (to be discussed in J. P. Stott et al. 2007, in preparation). We note that the poor constraints on the $f_{24}/f_{850}$ ratio mean that we cannot make robust conclusions about the rest-frame mid- to far-infrared differences between LAB 1a and LAB 2b. Both have $f_{24}/f_{850}$ upper limits consistent with obscured ULIRGs at $z \sim 3$ (Pope et al. 2006). Similarly, the limits of the observed $f_{5.8}/f_{850}$ ratios for LAB 1a and LAB 2b are consistent with other

---

[6] Vizier Online Data Catalog, 2255 (J. A. Surace et al., 2004).

[7] For mid-infrared detections within the Lyα halos, we adopt the alphabetical suffix LAB 1a, LAB 1b, etc., although this does not imply that these objects are physically associated with the LAB.

[8] LAB 2b is also at the location of the LBG M14, although in this case the LBG appears kinematically associated with the wider halo (Wilman et al. 2005). We note that in the submillimeter observation of this halo, LAB 2b is actually situated near to the edge of the SCUBA beam (Fig. 1). The correction to the 850 μm flux to account for this offset would make the SMG brighter, with $S_{850\,\mu m} \sim 5$ mJy (Chapman et al. 2001).
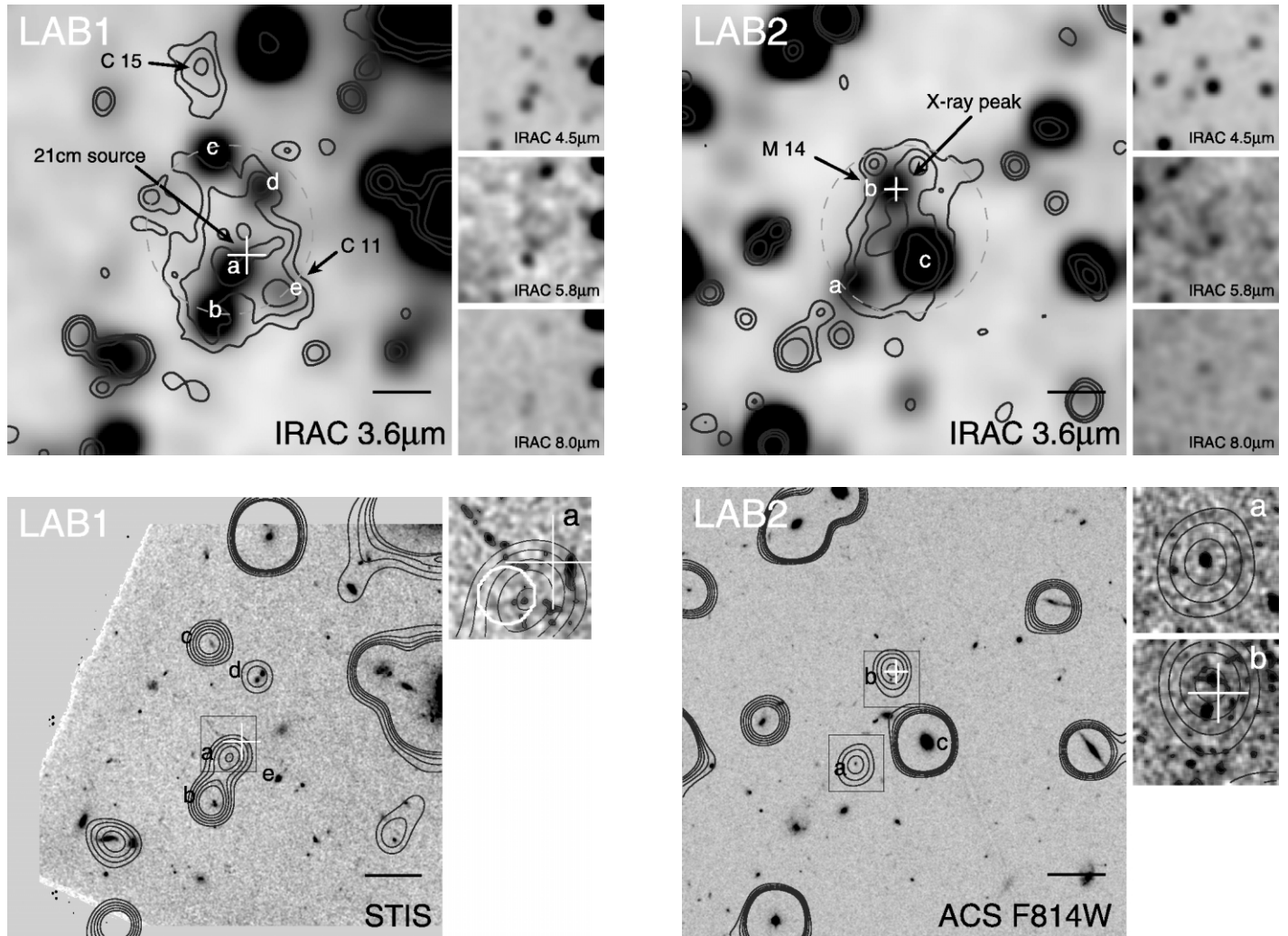
FIG. 1.—*Top*: Gray-scale IRAC 40″ × 40″ images of LAB 1 (*left*) and LAB 2 (*right*). The main panels show the IRAC 3.6 μm image, and the insets show the 4.5, 5.8, and 8 μm images, all of which have been slightly smoothed with a Gaussian kernel. We overlay the narrowband Lyα images from Matsuda et al. (2004) to show the extent of each halo. IRAC detections within the Lyα halos are labeled a, b, etc. In the field of LAB 1 we indicate the location of the known LBGs (C11 and C15) and the position of the 21 cm radio source in the halo (*white cross*; Chapman et al. 2004). LAB 2 contains one known LBG (M14) and an SMG, as well as an X-ray source (*white cross*). In both cases we show the 15″ SCUBA beam (*dashed circle*) to illustrate the potential uncertainty in the position of the submillimeter source. *Bottom*: High-resolution *HST* STIS and ACS imaging for LAB 1 and LAB 2 showing the optical counterparts, with contours showing the 3.6 μm emission. The white 1″ circle in the STIS inset shows the location of the ERO detected by Steidel et al. (2000). In all images north is up, east is left, and the horizontal bar is a 5″ scale. We discuss the identifications further in § 3 and Table 1. [*See the electronic edition of the Journal for a color version of this figure.*]

SMGs at $z \sim 3$, although the ratio for LAB 1a is at the low end of the distribution (Pope et al. 2006), indicating either a relatively low stellar mass for this system or, more likely, very high obscuration. Thus, the SMGs associated with LABs are similar to the wider SMG population.

We now examine the rest-frame near-infrared portion of the SEDs using the IRAC data. Near-infrared colors have been shown to be a useful diagnostic for the power source of local luminous infrared galaxies (e.g., Spinoglio et al. 1995). For LAB 1a we find rest-frame (Vega) colors $(J - H) = 0.6 \pm 0.5$ and $(H - K) = 0.8 \pm 0.4$, and in LAB 2b we find $(J - H) = 0.8 \pm 0.6$ and $(H - K) = 1.1 \pm 0.4$. LAB 1a's colors are similar to those of "normal" galaxies ($\langle J - H \rangle \sim 0.8$, $\langle H - K \rangle \sim 0.3$; Spinoglio et al. 1995), whereas LAB 2b exhibits a redder rest-frame $(H - K)$ color, indicating an excess in the rest-frame $K$-band likely associated with a nonstellar contribution. We fit a simple power law, $f_\nu \propto \nu^\alpha$, to the IRAC photometry for LAB 2b, obtaining $\alpha = -1.0 \pm 0.2$, similar to that expected for AGNs (Alonso-Herrero et al. 2006).

To further test whether the optical–mid-infrared SEDs of the sources can be reproduced by stellar populations, we use HYPERZ (Bolzonella et al. 2000) to model the stellar continuum by fitting to the rest-frame 0.15–2 μm photometry. We adopt a model with an exponentially declining star formation rate, with $\tau = 30$ Gyr, from Bruzual & Charlot (1993) and constrain the redshift to be $z = 3.09$. Dust is modeled with a Calzetti law (Calzetti et al. 2000). The rest-frame optical–near-infrared portions of the SEDs are well fit by this model, with high reddening ($A_V \sim 3$) and young ages. Absolute $K$-band magnitudes based on the fit are $M_K \sim -26.8$ in LAB 1a and $M_K \sim -27.2$ for LAB 2b. These absolute rest-frame $K$-band magnitudes are comparable to the wider SMG population (Borys et al. 2005) and suggest stellar masses of $M_\star \sim 10^{11}$ $M_\odot$, although the $K$-band magnitude of LAB 2b is likely to be contaminated by AGN emission, with a significant rest-frame 2 μm excess over the HYPERZ fit of ~5 μJy. The detection of X-ray emission from LAB 2b is the best evidence we have that it contains an AGN. To quantitatively test the
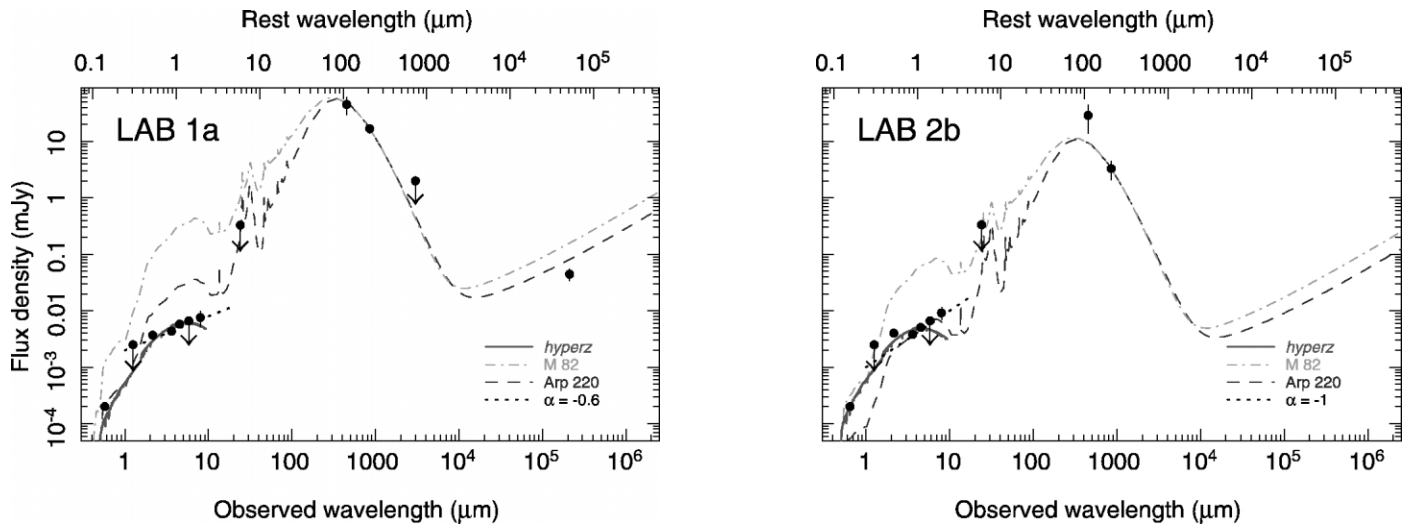
FIG. 2.—Rest-frame ultraviolet to radio SEDs of the proposed power sources in LAB 1 and LAB 2. We overlay the SEDs of M82 and Arp 220 (Silva et al. 1998) normalized to the 850 $\mu$m point and non-*Spitzer* data from the literature (upper limits at 3 $\sigma$). Both sources have broadband SEDs that are similar to Arp 220. Dotted lines show a simple power law, $f_\nu \propto \nu^\alpha$, fit to the 3.6–8 $\mu$m data. We also show the best fit (stellar) SED from HYPERZ, fitted to the optical/mid-infrared photometry (see § 4 for details). [*See the electronic edition of the Journal for a color version of this figure.*]

correspondence between the mid-infrared excess and the X-ray emission, we use the rest-frame X-ray–10.5 $\mu$m correlation for AGNs from Krabbe et al. (2002). We predict the rest-frame 10.5 $\mu$m emission for LAB 2b by extrapolating the rest-frame 2 $\mu$m using the measured spectral slope of $\alpha = -1$. With this approach we estimate the X-ray luminosity from the AGN to be of order $10^{44}$ ergs s$^{-1}$, in reasonable agreement with that observed (Basu-Zych & Scharf 2004). The luminosity of the X-ray source is consistent with a moderate contribution to the bolometric emission from an AGN (Alexander et al. 2005a); however, it is still not clear whether an AGN or starburst is responsible for powering the extended Ly$\alpha$ emission. LAB 1a's rest-frame $K$-band excess of $\sim 3 \pm 2$ $\mu$Jy over the best-fit stellar template is less significant. Nevertheless, taking the same approach as for LAB 2b, we predict an X-ray luminosity of $\sim 5 \times 10^{43}$ ergs s$^{-1}$, consistent with the 2–10 keV limit in the existing *Chandra* observations.

To make progress we need mid-infrared observations of a larger sample of LABs in SA 22, four of which also contain SMGs (Geach et al. 2005). This will allow us to investigate whether they also exhibit rest-frame near-infrared characteristics similar to the general submillimeter population. Searches for obscured AGNs in SA 22 will also be significantly advanced by a recently approved 400 ks *Chandra* ACIS-I exposure of this region. Together these studies will provide a clearer view of the energetics of LABs and their relationship to the wider SMG population.

## REFERENCES

Alexander, D. M., Bauer, F. E., Chapman, S. C., Smail, I., Blain, A. W., Brandt, W. N., & Ivison, R. J. 2005a, ApJ, 632, 736
Alexander, D. M., Smail, I., Bauer, F. E., Chapman, S. C., Blain, A. W., Brandt, W. N., & Ivison, R. J. 2005b, Nature, 434, 738
Alonso-Herrero, A., et al. 2006, ApJ, 640, 167
Ashby, M. L. N., et al. 2006, ApJ, 644, 778
Basu-Zych, A., & Scharf, C. 2004, ApJ, 615, L85
Bertin, E., & Arnouts, S. 1996, A&AS, 117, 393
Bolzonella, M., Miralles, J.-M., & Pello, R. 2000, A&A, 363, 476
Borys, C., Smail, I., Chapman, S. C., Blain, A. W., Alexander, D. M., & Ivison, R. J. 2005, ApJ, 635, 853
Bower, R. G., et al. 2004, MNRAS, 351, 63
Bruzual, G., & Charlot, S. 1993, ApJ, 405, 538
Calzetti, D., Armus, L., Bohlin, R. C., Kinney, A. L., Koorneef, J., & Storchi-Bergmann, T. 2000, ApJ, 533, 682
Chapman, S. C., Lewis, G. F., Scott, D., Richards, E., Borys, C., Steidel, C. C., Adelberger, K. L., & Shapley, A. E. 2001, ApJ, 548, L17
Chapman, S. C., Scott, D., Windhorst, R. A., Frayer, D. T., Borys, C., Lewis, G. F., & Ivison, R. J. 2004, ApJ, 606, 85
Francis, P. J., et al. 2001, ApJ, 554, 1001

Geach, J. E., et al. 2005, MNRAS, 363, 1398
Keel, W. C., Cohen, S. H., Windhorst, R. A., & Waddington, I. 1999, AJ, 118, 2547
Krabbe, A., Böker, T., & Maiolino, R. 2002, in ASP Conf. Ser. 258, Issues in Unification of Active Galactic Nuclei, ed. R. Maiolino, A. Marconi, & N. Nagar (San Francisco: ASP), 33
Matsuda, Y., et al. 2004, AJ, 128, 569
Ohyama, Y., et al. 2003, ApJ, 591, L9
Palunas, P., Teplitz, H. I., Francis, P. J., Williger, G. M., & Woodgate, B. E. 2004, ApJ, 602, 545
Pope, A., et al. 2006, MNRAS, 370, 1185
Reuland, M., et al. 2003, ApJ, 592, 755
Scharf, C. A., et al. 2003, ApJ, 596, 105
Silva, L., Granato, G. L., Bressan, A., & Danese, L. 1998, ApJ, 509, 103
Spinoglio, L., Malkan, M. A., Ruch, B., Carrasco, L., & Recillas-Cruz, E. 1995, ApJ, 453, 616
Steidel, C., et al. 2000, ApJ, 532, 170
Taniguchi, T., & Shioya, Y. 2000, ApJ, 532, L13
Wilman, R. J., et al. 2005, Nature, 436, 227